

Optimal orientation detection of an anisotropic dipolar scatterer

Felix Tebbenjohanns,^{1,2} Andrei Militaru,¹ Andreas Norrman,^{1,3}
Fons van der Laan,¹ Lukas Novotny,^{1,4} and Martin Frimmer¹

¹*Photonics Laboratory, ETH Zürich, CH-8093 Zürich, Switzerland*

²*Department of Physics, Humboldt-Universität zu Berlin, 10099 Berlin, Germany*

³*Institute of Photonics, University of Eastern Finland, P.O. Box 111, FI-80101 Joensuu, Finland*

⁴*Quantum Center, ETH Zürich, CH-8093 Zürich, Switzerland*

(Dated: September 20, 2021)

The angular orientation of an anisotropic scatterer with cylindrical symmetry in a linearly polarized light field represents an optomechanical libration. Here, we propose and theoretically analyze an optimal measurement scheme for the two angular degrees of freedom of such a libration and demonstrate that this scheme reaches the Heisenberg limit of the imprecision-backaction product. Furthermore, we propose and analyze a realistic measurement scheme and show that measurement-based ground-state cooling of the rotational degrees of freedom of an anisotropic point scatterer levitated in an optical trap is feasible.

I. INTRODUCTION

At the heart of optomechanics lies the task to measure and control mechanical motion using light [1]. To a large extent, the optomechanics community has focused on translational degrees of freedom, such as the position of a mirror [2, 3], or the position of a particle in an optical trap [4]. Recently, rotational degrees of freedom of anisotropic particles levitated in optical and radiofrequency traps have attracted significant attention [5–9]. A dumbbell, composed of two identical spherical particles in touching contact, is an example of an anisotropic scatterer. In a linearly polarized laser field, dumbbells align with their long axis along the polarization direction due to the exerted optical torque. For small angular deviations around the equilibrium position, this angular motion represents a harmonic oscillator degree of freedom, termed libration. Gaining quantum control of these libration modes is an exciting prospect [10], since it may allow the investigation of quantum coherent evolution of the rotational degrees of freedom of macroscopic objects [11–13]. Accordingly, a quantum toolbox of rotational motion may provide an avenue that complements current efforts to investigate macroscopic superposition states using the center-of-mass motion of levitated particles [14]. Another prospect of optically levitated rotors is to harness them as torque sensors to investigate elusive physics of rotating bodies, such as the rotational Casimir effect and vacuum friction [15–18]. Developing levitated librators into a quantum resource can take inspiration from the measurement and control schemes developed for center-of-mass modes [19, 20]. One of the crucial ingredients for quantum control of these modes has been the optimization of their optical detection [21]. While first steps to measure and feedback-control the libration modes of levitated nanoparticles have been taken [8, 22], an understanding of the optimal detection process for the orientation of an optically levitated dumbbell is still missing.

In this paper, we analyze the detection of the librational

motion of a lossless dipolar point scatterer with cylindrical symmetry (such as a dielectric nanodumbbell) in a linearly polarized laser field. First, we propose and theoretically analyze an ideal detection system to measure both angular degrees of freedom. We show that the imprecision-backaction product of our measurement scheme reaches the Heisenberg limit and is thus optimal. Second, we propose and analyze a realistic detection scheme that has the potential to allow for measurement-based ground-state cooling of librational motion.

II. SYSTEM UNDER INVESTIGATION

Throughout this work, we consider an absorption-free anisotropic dipolar point scatterer with cylindrical symmetry described by its polarizability tensor α . For a scatterer with vanishing material loss in the optical frequency range of interest, the imaginary part of the polarizability (which is due to radiation loss) is negligible for our purposes, such that α can be taken as purely real. In a frame of reference with the x axis aligned with the scatterer's symmetry axis, the polarizability takes the form $\alpha = \text{diag}[\alpha_x, \alpha_z, \alpha_z]$ [23]. An example of such a scatterer of particular practical relevance is the workhorse of rotational optomechanics, a dumbbell composed of two touching subwavelength spheres, as illustrated in Fig. 1(a). The scatterer is irradiated by a light field (angular frequency ω_0), which is linearly polarized along x at the location of the scatterer and has amplitude E_0 . We note that only the driving field at the scatterer position is of relevance and the mode shape of the driving field plays no role. The scatterer experiences a torque aligning its long axis with the polarization direction of the field. In this aligned situation, the dipole moment induced in the scatterer by the driving field points purely along the x direction and is given by $p_x = \alpha_x E_0$. We are interested in measuring the angular deviation of the scatterer's orientation from this equilibrium position.

For small angular deviations, the orientation of the scatterer is fully described by two angles δ and ϵ , where δ denotes a rotation of the scatterer around the z axis, and ϵ around the $-y$ axis, as illustrated in Fig. 1(b). For small angles δ and ϵ , the order in which these rotations are effected is irrelevant. To linear order, a tilt by ϵ gives rise to an induced dipole moment along the z axis $p_z = \epsilon \Delta\alpha E_0$, where $\Delta\alpha = \alpha_x - \alpha_z$ characterizes the anisotropy of the scatterer. With the dipole moment along the polarization direction p_x , we can thus write $p_z = \epsilon(\Delta\alpha/\alpha_x)p_x$. Analogously, a tilt by δ gives rise to a dipole moment along the y direction with amplitude $p_y = \delta(\Delta\alpha/\alpha_x)p_x$.

III. IDEAL MEASUREMENT SYSTEM

The central question answered in this paper is: How can we optimally infer the orientation of the anisotropic scatterer (i.e., the angles δ and ϵ) in a linearly polarized electromagnetic field? In other words, we seek to determine the orientation of a radiating dipole with dipole moment \mathbf{p} by analyzing its radiation field.

In complex notation, the far-field generated by the dipole $\mathbf{p} = [p_x, p_y, p_z]$ is given by a superposition of the field generated by each component of the dipole as

$$\mathbf{E}_{\text{sc}} = \sqrt{P_0} \left(\mathbf{e}^{(x)} + \delta \frac{\Delta\alpha}{\alpha_x} \mathbf{e}^{(y)} + \epsilon \frac{\Delta\alpha}{\alpha_x} \mathbf{e}^{(z)} \right). \quad (1)$$

Here, $\mathbf{e}^{(i)}$ with $i \in \{x, y, z\}$ are the dipolar modes given by [24]

$$\mathbf{e}^{(i)} = \sqrt{\frac{3}{8\pi}} [(\mathbf{n}_i \cdot \mathbf{n}_\theta) \mathbf{n}_\theta + (\mathbf{n}_i \cdot \mathbf{n}_\phi) \mathbf{n}_\phi], \quad (2)$$

where \mathbf{n}_θ is the unit vector along the polar direction (relative to the z axis), \mathbf{n}_ϕ the one along the azimuthal direction, and \mathbf{n}_i are the Cartesian unit vectors. These dipolar modes are orthogonal in the sense that

$$\int d\Omega \mathbf{e}^{(i)} \cdot \mathbf{e}^{(j)} = \delta_{ij}, \quad (3)$$

where the integral is over the full solid angle and δ_{ij} denotes the Kronecker delta. We have normalized the field \mathbf{E}_{sc} such that integration of its modulus squared over the full solid angle yields the total scattered power $P_0 = \omega_0^4 \alpha_x^2 E_0^2 / (12\pi \epsilon_0 c^3)$, which is independent of δ and ϵ to linear order. Here, ϵ_0 is the vacuum permittivity and c the speed of light in vacuum. According to Eq. (1), the information about the angles δ and ϵ is encoded in the amplitudes of the $\mathbf{e}^{(y)}$ and $\mathbf{e}^{(z)}$ dipolar modes, respectively. In order to extract these amplitudes, and infer the scatterer's orientation, we use the homodyne detection scheme illustrated in Fig. 1(c). In this scheme, we combine the signal field \mathbf{E}_{sc} with a local oscillator (LO) field, with an amplitude much larger than that of the signal. In App. A, we

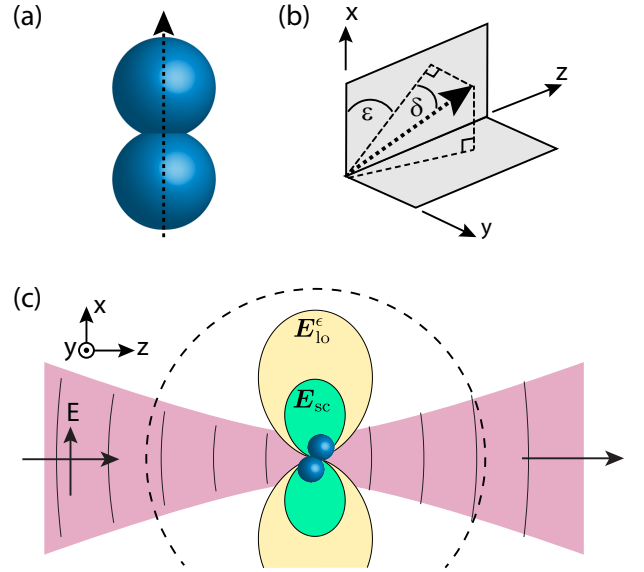


Figure 1. (a) Asymmetric scatterer with cylindrical symmetry depicted as a dumbbell composed of two touching spheres. The orientation of the dumbbell is described by the orientation of its axis of symmetry, illustrated by the dashed arrow. (b) Illustration of coordinate system. The laboratory frame is described by the Cartesian coordinate axes x , y , and z . The orientation of the dumbbell (shown as the dashed arrow) can be described by the orientation of its symmetry axis relative to the Cartesian axes. Small deviations of this symmetry axis from the Cartesian x axis can be described by the rotation angle δ around the z axis, and the rotation angle ϵ around the $-y$ axis. (c) Illustration of optimal detection scheme for the angle ϵ . The dumbbell is driven by an x -polarized field, exemplarily illustrated in red as a beam of light traveling along the z axis. The tilt by ϵ gives rise to an induced dipole moment along z . The field \mathbf{E}_{sc} generated by that z -oriented dipole (illustrated in green) populates the mode $\mathbf{e}^{(z)}$. For optimal detection, that scattered field is mixed with a strong local oscillator field $\mathbf{E}_{\text{lo}}^\epsilon$ in the same dipolar radiation mode (illustrated in yellow). The field intensity is measured on a 4π detector, illustrated as the dashed black line.

show explicitly that an LO field in the same mode as the signal field maximizes the signal-to-noise ratio on the detector. Thus, we choose

$$\mathbf{E}_{\text{lo}}^\delta = \sqrt{P_{\text{lo}}} \mathbf{e}^{(y)} \quad (4)$$

as our LO field for measuring δ and $\mathbf{E}_{\text{lo}}^\epsilon = \sqrt{P_{\text{lo}}} \mathbf{e}^{(z)}$ for measuring ϵ . To keep our discussion of the ideal measurement scheme accessible, we consider a measurement of either δ or ϵ at one time. Nevertheless, we stress that one can, in principle, measure both angles simultaneously, since their associated radiation modes are orthogonal according to Eq. (3).

The power measured by our detector dedicated to the angle δ then reads

$$P_{\text{det}}^\delta = \int d\Omega |\mathbf{E}_{\text{lo}}^\delta + \mathbf{E}_{\text{sc}}|^2 = P_{\text{lo}} + 2\sqrt{P_{\text{lo}}P_0} \frac{\Delta\alpha}{\alpha_x} \delta, \quad (5)$$

where we assumed $P_0 \ll P_{\text{lo}}$. The signal P_{det}^δ indeed pro-

vides a linear measurement of the orientation angle δ , as desired. An analogous calculation for P_{det}^ϵ yields an expression identical to Eq. (5), with δ replaced by ϵ . Assuming that the noise on our detector is dominated by photon shot noise with power spectral density $S_{PP} = (2\pi)^{-1}\hbar\omega_0 P_0$ (with \hbar the reduced Planck constant and ω_0 the optical frequency) [25], we find the measurement imprecision

$$S_{\delta\delta} = S_{\epsilon\epsilon} = \frac{1}{2\pi} \left(\frac{\alpha_x}{\Delta\alpha} \right)^2 \frac{\hbar\omega_0}{4P_0}. \quad (6)$$

Here $S_{\delta\delta}$ and $S_{\epsilon\epsilon}$ denote the power spectral densities (PSD) of the measurements of δ and ϵ , respectively [26]. In App. A, we provide a generalized treatment for the measurement imprecision of any linear measurement limited by photon shot noise.

With Eq. (6), we have derived the measurement imprecision of our detection scheme for the angular orientation of an anisotropic dipolar scatterer in a linearly polarized electromagnetic field. Equation (6) shows that the imprecision noise scales inversely with the number of photons scattered per unit time, which is given by $P_0/(\hbar\omega_0)$. This behavior is well known for any linear measurement limited by photon shot noise. Furthermore, the imprecision noise scales inversely with the (square of the) optical anisotropy $\Delta\alpha$. Indeed, for an isotropic scatterer with $\Delta\alpha = 0$, the measurement imprecision diverges since the scattered field cannot provide any information about the scatterer's orientation.

IV. MEASUREMENT BACKACTION

Having determined the imprecision of our measurement scheme for the orientation angles δ and ϵ of the anisotropic scatterer, we now turn to an analysis of the measurement backaction. This backaction arises as a torque noise driving the rotational motion of the scatterer and has been derived earlier [23, 27, 28]. To make this article self contained, we provide a particularly simple and didactic treatment here.

The system under consideration is still the anisotropic scatterer with polarizability $\alpha = \text{diag}[\alpha_x, \alpha_z, \alpha_z]$, aligned with its long axis to an x -polarized electric driving field, as outlined in Sec. II. The instantaneous torque $\tau(t)$ experienced by a dipole moment $\mathbf{p}_{\text{tot}}(t)$ interacting with an electric field $\mathbf{E}_{\text{tot}}(t)$ is given by [29]

$$\boldsymbol{\tau}(t) = \mathbf{p}_{\text{tot}}(t) \times \mathbf{E}_{\text{tot}}(t). \quad (7)$$

Throughout this section, $\mathbf{p}_{\text{tot}}(t)$ and $\mathbf{E}_{\text{tot}}(t)$ are real valued, time dependent quantities. We split the electric field into the deterministic driving field $\mathbf{E}(t) = E_0 \cos(\omega_0 t) \mathbf{n}_x$, and a fluctuating background field $\tilde{\mathbf{E}}(t) = [\tilde{E}_x(t), \tilde{E}_y(t), \tilde{E}_z(t)]$, such that the total field reads $\mathbf{E}_{\text{tot}}(t) = \mathbf{E}(t) + \tilde{\mathbf{E}}(t)$. Throughout this work, we denote fluctuating quantities with a tilde and assume them

to be statistically stationary, random variables of zero-mean. When the scatterer is in its equilibrium position with $\delta = \epsilon = 0$, the total dipole moment can be written as $\mathbf{p}_{\text{tot}}(t) = \alpha \mathbf{E}_{\text{tot}}$, where we approximated the polarizability α as purely real and given by its value at the optical frequency ω_0 . We are interested in the fluctuating optical torque $\tilde{\boldsymbol{\tau}}(t)$, which to first order in the field fluctuations reads

$$\begin{aligned} \tilde{\boldsymbol{\tau}}(t) &= \alpha_x \mathbf{E}(t) \times \tilde{\mathbf{E}}(t) + [\alpha \tilde{\mathbf{E}}(t)] \times \mathbf{E}(t) \\ &= E_0 \Delta\alpha \cos(\omega_0 t) \begin{pmatrix} 0 \\ -\tilde{E}_z(t) \\ \tilde{E}_y(t) \end{pmatrix}. \end{aligned} \quad (8)$$

We thus find for the PSD of the y component of the torque fluctuations $\tilde{\tau}_y$

$$\begin{aligned} S_{\tau\tau}^{yy}(\omega) &= \frac{1}{2\pi} \int_{-\infty}^{\infty} dt' \langle \tilde{\tau}_y(t+t') \tilde{\tau}_y(t) \rangle e^{i\omega t'} \\ &= \frac{E_0^2}{4} (\Delta\alpha)^2 [S_{EE}^{zz}(\omega + \omega_0) + S_{EE}^{zz}(\omega - \omega_0)], \end{aligned} \quad (9)$$

where $S_{EE}^{zz}(\omega)$ is the PSD of \tilde{E}_z and the angle brackets denote ensemble and time average. An analogous expression is obtained for $S_{\tau\tau}^{zz}(\omega)$, which depends on $S_{EE}^{yy}(\omega)$. Note that in our derivation $\tilde{\boldsymbol{\tau}}(t)$ and $\tilde{\mathbf{E}}(t)$ could be both Hermitian quantum operators or classical, real-valued random processes with PSDs $S_{\tau\tau}^{ii}(\omega)$ and $S_{EE}^{ii}(\omega)$, $i \in \{x, y, z\}$, respectively. In both cases, in the experimentally accessible regime of $|\omega| \ll \omega_0$, the PSDs of the torque fluctuations arise from the symmetric part of the field PSDs, which in vacuum are given by [30, 31]

$$S_{EE}^{ii}(\omega_0) = S_{EE}^{ii}(-\omega_0) = \frac{\hbar|\omega_0|^3}{12\pi^2\epsilon_0 c^3}. \quad (10)$$

In quantum theory, these field fluctuations can be seen as a consequence of the fact that the ladder operators describing the electromagnetic field do not commute [30]. In the framework of stochastic electrodynamics, these correlations are postulated to originate from a classical electromagnetic background field chosen such that each mode at frequency ω carries energy $\hbar\omega/2$ [31, 32]. With these correlations for the fluctuating fields, the scattered power $P_0 = \omega_0^4 \alpha_x^2 E_0^2 / (12\pi\epsilon_0 c^3)$, and the assumption $|\omega| \ll \omega_0$, the PSDs of the fluctuating torque components $\tilde{\tau}_y$ and $\tilde{\tau}_z$ read

$$S_{\tau\tau}^{yy} = S_{\tau\tau}^{zz} = \frac{1}{2\pi} \left(\frac{\Delta\alpha}{\alpha_x} \right)^2 \hbar^2 \frac{P_0}{\hbar\omega_0}. \quad (11)$$

The x component of the torque fluctuations vanishes, according to Eq. (8), such that we have $S_{\tau\tau}^{xx}(\omega) = 0$. For a rotor with inertial moment I , the torque noise PSD in Eq. (11) translates into a rotational energy heating rate

$\dot{E} = \pi S_{\tau\tau}/I$ [25, 33]. We note that our result Eq. (11) matches the one of Ref. [28].

Let us interpret Eq. (11). The measurement backaction is proportional to the total number of photons scattered per unit time, $P_0/(\hbar\omega_0)$, since the photons are the source of the torque recoil. Since each photon carries an angular momentum of \hbar , the measurement backaction (which scales with the torque variance) is proportional to \hbar^2 . Finally, the (square of the) optical anisotropy $\Delta\alpha/\alpha_x$ enters Eq. (11), since an optical field cannot exert any torque on a lossless scatterer with vanishing anisotropy.

As a side, we note that our treatment provides an interesting insight into the role of classical noise, which may be present in the driving laser. Such classical laser noise would increase \tilde{E}_x beyond the level set by the vacuum fluctuations in Eq. (10). Interestingly, while the (vacuum) fluctuations in the y and z components of the electric field dominate the torque fluctuations according to Eq. (8), driving laser fluctuations \tilde{E}_x make no appearance, such that classical laser noise does not lead to torque noise to linear order. For this reason, optomechanical systems based on levitated dipolar scatterers are particularly resilient to classical laser noise.

As a further side note, our treatment provides some fundamental insight on how to engineer the torque shot noise acting on the anisotropic scatterer. Equation (8) shows that $\tilde{\tau}_y$ depends exclusively on the vacuum fluctuations along the z direction \tilde{E}_z at the origin. To understand how to gain full control over that field component, it is instructive to consider the field impinging onto the scatterer in an expansion into vector spherical harmonics [34, 35]. In this basis, the only mode leading to a finite electric field along z at the origin is the dipole mode $e^{(z)}$. Therefore, it is the noise in this mode only, which heats the libration angle ϵ . To modify most efficiently the shot noise heating of this libration mode using squeezing, one therefore must feed squeezed vacuum into the incoming $e^{(z)}$ mode. The effect of squeezing any other mode, e.g., the trapping beam, is limited by its mode overlap with $e^{(z)}$. In analogy, for efficient suppression of shot noise heating of the angle δ , the dipolar mode $e^{(y)}$ must be squeezed.

Returning to our problem of optimal orientation detection, let us review our findings so far. In Sec. III, we have computed the measurement imprecision of our optimal measurement scheme for the angles δ and ϵ , given by Eq. (6). In the current Section, we have derived the measurement backaction Eq. (11) experienced by the scatterer due to the interference of the strong driving field with the electromagnetic vacuum fluctuations. Importantly, the product between the measurement imprecision and the backaction yields the Heisenberg limit according to [25]

$$S_{\tau\tau}^{zz} \times S_{\delta\delta} = S_{\tau\tau}^{yy} \times S_{\epsilon\epsilon} = \frac{1}{4\pi^2} \frac{\hbar^2}{4}. \quad (12)$$

Thus, the measurement scheme presented in Sec. III indeed

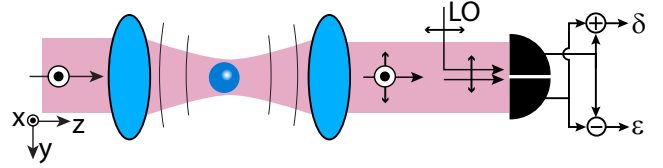


Figure 2. Realistic detection scheme. A dumbbell (long axis along x) is trapped in an x -polarized field. The scattered field is collected in the forward direction and mixed with a strong y polarized local oscillator (LO) before it is measured on a detector split in two halves along the xz plane. The sum signal gives access to the orientation angle δ , while the difference signal is proportional to the angle ϵ of the dumbbell.

represents an optimal scheme to resolve the angular orientation of the scatterer.

V. REALISTIC MEASUREMENT SCHEME

The measurement scheme presented in Sec. III has been proven to be ideal, albeit it is hardly practical. In this section, we analyze a simple and thus realistic detection scheme and quantify its efficiency. In our realistic scenario, illustrated in Fig. 2, the scatterer is again trapped by an x polarized beam propagating along the positive z axis. The trapping beam is focused by a trapping lens and recollimated by a collection lens. These lenses also collect the scattered light. According to Eq. (1), the information about the orientation angles δ and ϵ is contained in dipolar radiation modes which are symmetric with respect to the xy plane. Therefore, detection in the forward and backward direction yields equal detection efficiency. Here, we choose to place our detector in the forward direction, but we note that the treatment of the scheme in backscattering is analogous. The field collimated by the collection lens is interfered with a strong y polarized reference field serving as a local oscillator (LO). This LO field is assumed to be spatially homogeneous across the numerical aperture of the collection lens and in-phase with the signal field.

We stress that it is far from optimal to harness the transmitted trapping beam as a local oscillator. Our objective is to determine the amplitude of the scattered field, which encodes the orientation angles δ and ϵ . However, due to the Gouy phase shift in a focused field, the scattered field and the transmitted trapping beam are in different quadratures and therefore set up to detect the phase of the signal field, not its amplitude [36]. The transmitted trapping beam thus only generates shot noise on the detector, without providing any information to linear order. When detecting in the forward direction, one should therefore either dump the trapping beam with a polarizing beamsplitter, or use a LO which is much stronger than the transmitted trapping beam, as we assume in our discussion and in Fig. 2.

For mathematical convenience, we treat the interference

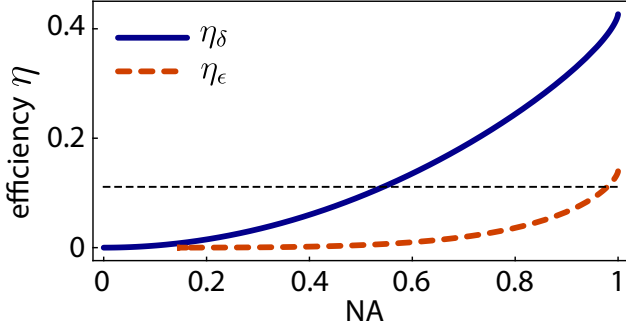


Figure 3. Detection efficiencies η_δ (blue solid line) and η_ϵ (orange dashed line) of our realistic detection scheme according to Eqs. (14) and (16) as a function of the numerical aperture (NA) of the collection lens. The black dashed horizontal line marks $\eta = 1/9$, the detection efficiency required to feedback cool to a phonon occupation number $n = 1$.

of the LO field with the scattered field on the reference sphere of the collection lens, where the LO field reads [24]

$$\mathbf{E}_{\text{lo}} = \sqrt{\frac{P_{\text{lo}}}{\pi \text{NA}^2}} \cos \theta [\sin \phi \mathbf{n}_\theta + \cos \phi \mathbf{n}_\phi]. \quad (13)$$

We use the complex notation and normalization introduced in Sec. III, such that integration of the LO field's modulus squared over the reference sphere within the numerical aperture $\text{NA} = \sin \theta_m$ (given by the maximum collection angle θ_m) yields the total power in the LO beam P_{lo} .

To quantify the performance of our realistic measurement scheme for the angle δ , we must analyze its imprecision noise $S_{\delta\delta}^{\text{re}}$ and compare it to that of the ideal measurement $S_{\delta\delta}$, given by Eq. (6). The relevant figure of merit is thus the detection efficiency $\eta_\delta = S_{\delta\delta}/S_{\delta\delta}^{\text{re}}$. An analogous treatment must be carried out for the angle ϵ . As detailed in App. A, the detection efficiencies associated with the measurements of δ and ϵ are given by the overlap integral between the chosen LO field Eq. (13) and the signal field Eq. (1). According to Eq. (A8), we find for the angle δ the detection efficiency

$$\eta_\delta = \frac{1}{P_{\text{lo}}} \left(\int d\Omega \mathbf{e}^{(y)} \cdot \mathbf{E}_{\text{lo}} \right)^2 = \frac{3U^2}{8\pi^2 \text{NA}^2}, \quad (14)$$

with

$$\begin{aligned} U(\theta_m) &= \int_0^{2\pi} d\phi \int_0^{\theta_m} d\theta \sin \theta \sqrt{\cos \theta} \\ &\quad \times [\cos \theta \sin^2 \phi + \cos^2 \phi] \\ &= \frac{2\pi}{15} \left[8 - \cos^{\frac{3}{2}}(\theta_m)(3 \cos \theta_m + 5) \right]. \end{aligned} \quad (15)$$

In Fig. 3, we plot the detection efficiency η_δ as a function of numerical aperture as the solid blue line. To quantify the price we pay for the practicability of the realistic detection scheme, it is instructive to consider the detection efficiency

for an NA of unity, where we find $\eta_\delta^{\text{max}} = 32/75$. This result is remarkably close to the value of one half, provided by ideal detection in a single half space. The deviation from the optimal result arises from the imperfect overlap of the LO field (a plane wave) with the signal field (radiation field of a dipole).

Having analyzed the detection efficiency for the angle δ , let us turn to the angle ϵ , which is encoded in the mode $\mathbf{e}^{(z)}$, whose field strictly points along \mathbf{n}_θ . When projected onto the local oscillator Eq. (13), the overlap integral contains the term $\sin \phi$, such that integration of ϕ over the domain $[0 \dots 2\pi]$ yields a vanishing signal. Therefore, we split the detector into an ‘‘upper’’ half in the range $\phi = [0 \dots \pi]$, and a ‘‘lower’’ half corresponding to $\phi = [-\pi \dots 0]$. While summing the signals from these two halves leads to the detection of the angle δ , as discussed, subtracting the signals provides access to the angle ϵ . We thus find for the detection efficiency of the angle ϵ

$$\eta_\epsilon = \frac{6V^2}{\pi^2 \text{NA}^2}, \quad (16)$$

with

$$V(\theta_m) = \int_0^{\theta_m} d\theta \sin^2 \theta \sqrt{\cos \theta}. \quad (17)$$

We plot η_ϵ as the orange dashed line in Fig. 3. We note that η_ϵ is consistently lower than η_δ . This observation can be explained by two reasons. First, the angle ϵ gives rise to a dipole moment induced in the scatterer pointing along z . This dipole radiates predominantly into the xy plane, such that the signal is poorly captured by a collection optic of finite numerical aperture positioned along the z axis. Second, even at unity numerical aperture, the overlap of the y -polarized LO field (or any other linearly polarized LO field) with the radiation mode $\mathbf{e}^{(z)}$ of the z dipole is rather poor.

It is possible to double the detection efficiency for ϵ in the forward direction by splitting the field at a polarizing beamsplitter into the y component (and interfering it with a y polarized local oscillator as just discussed), and the x component, which has to be interfered with an x -polarized local oscillator. Due to the symmetry of the problem, the detector for the x component should be split into a ‘‘left’’ and a ‘‘right’’ half. As already mentioned, a technical difficulty arises in forward scattering from the fact that the transmitted trapping field is x -polarized, such that the local oscillator in that polarization direction has to be much stronger than the trapping field. In backscattering, this technical problem is absent.

Let us discuss the consequences of our findings for measurement-based quantum control of libration modes of levitated nanoparticles. In a regime where the dominant heating rate is due to measurement backaction, linear feedback control allows for cooling a harmonic oscillator to a mean phonon occupation $n = [\eta^{-1/2} - 1]/2$, only limited

by the detection efficiency η [3]. Accordingly, cooling to unity phonon occupation (regarded as “ground-state cooling” by the community) requires a detection efficiency of $1/9$, which is marked as the black dashed horizontal line in Fig. 3. At a realistically achievable numerical aperture of 0.9, we find for the angle ϵ a detection efficiency $\eta_\epsilon = 0.07$ and an associated phonon occupation $n_\epsilon = 1.4$. For the angle δ , we find $\eta_\delta = 0.31$, allowing for cooling to a phonon occupation $n_\delta = 0.4$. Therefore, cooling the δ libration mode to its quantum ground state appears feasible with our realistic detection scheme. One should keep mind that our estimation is rather conservative given that the detection efficiencies plotted in Fig. (3) can be significantly improved with some additional technical overhead. The efficiency η_δ can be doubled by implementing both a forward and a backward detection system. Furthermore, the efficiency η_ϵ plotted in Fig. (3) can be quadrupled by implementing both a forward and a backward detection system and analyzing both polarization components. Therefore, regarding the performance of a feasible detection scheme, ground-state cooling of librational motion appears within experimental reach.

VI. CONCLUSION

In conclusion, we have theoretically analyzed the problem of measuring the orientation of an asymmetric scatterer with cylindrical symmetry in a linearly polarized light field. We have devised an optimal detection scheme for each of the two angles describing the scatterer’s orientation, and we have analyzed the associated measurement imprecision. To prove that our measurement scheme is optimal, we have derived the associated measurement backaction and demonstrated that the imprecision-backaction product meets the Heisenberg limit. Furthermore, we have proposed and analyzed a realistic detection scheme. The efficiency of our realistic and simple measurement scheme is sufficient to allow for measurement-based feedback cooling of one angular degree of freedom of an anisotropic optically levitated particle to its quantum ground state of motion. With some additional technical overhead, ground-state cooling of both angular degrees of freedom is within reach.

ACKNOWLEDGMENTS

We acknowledge financial support by ETH Grant ETH-47 20-2. A.N. thanks the Jane and Aatos Erkko Foundation (Finland) for funding.

Appendix A: Generalized linear measurement

In this Appendix, we treat the case of a generalized linear measurement. First, we determine the optimal local oscillator (LO) field to extract a scalar quantity linearly encoded in a signal field. Second, we derive the measurement imprecision of such a generalized linear measurement in the presence of photon shot noise in the case of an optimal and a sub-optimal LO field.

Suppose that a dimensionless quantity x is linearly encoded in a signal field given by $x\mathbf{E}_s(\Omega)$. This quantity x could, for example, be one of the angles δ or ϵ in the main text. Assume that this signal field strikes a detector surface $A(\Omega)$, which is parametrized by Ω , at normal incidence. A LO field $\mathbf{E}_{10}(\Omega)$ is superposed with the signal field to interfere on the detector. Let this LO field carry a total power $P_{10} = \int_A d\Omega \mathbf{E}_{10}^* \cdot \mathbf{E}_{10}$, where the asterisk denotes complex conjugation. Note that throughout this appendix, as in Secs. III and V, all fields are expressed in complex notation and normalized such that integration of their modulus squared over solid angle yields their power. The detector signal fluctuates due to photon shot noise. We now show that in order to minimize the measurement imprecision for x , the field distribution $\mathbf{E}_{10}(\Omega)$ must be in the same mode as the signal field $\mathbf{E}_s(\Omega)$.

We start with the power P received by our detector

$$P = \int_A d\Omega |\mathbf{E}_{10} + x\mathbf{E}_s|^2 = P_{10} + Cx, \quad (\text{A1})$$

where we expanded to first order in the signal field and introduced the calibration factor C , which converts our signal from units of x to units of power

$$C = 2 \int_A d\Omega \text{Re} [\mathbf{E}_{10}^* \cdot \mathbf{E}_s]. \quad (\text{A2})$$

The detected power P has a constant offset P_{10} and an interference term Cx , and therefore represents a linear measurement of the quantity x . The power fluctuations due to photon shot noise of the dominating power P_{10} have a white noise floor with power spectral density (PSD)

$$S_{PP} = \frac{\hbar\omega_0}{2\pi} P_{10}, \quad (\text{A3})$$

such that the PSD of the imprecision noise of x is

$$S_{xx} = \frac{S_{PP}}{C^2}. \quad (\text{A4})$$

We now express both the LO field $\mathbf{E}_{10} = \sqrt{P_{10}}\mathbf{e}_{10}$ and the signal field $\mathbf{E}_s = \sqrt{P_s}\mathbf{e}_s$ with their respective mode functions \mathbf{e}_{10} and \mathbf{e}_s , which are normalized according to

$$\int_A d\Omega \mathbf{e}_{10}^* \cdot \mathbf{e}_{10} = \int_A d\Omega \mathbf{e}_s^* \cdot \mathbf{e}_s = 1. \quad (\text{A5})$$

With the power of the signal field $P_s = \int_A d\Omega \mathbf{E}_s^* \cdot \mathbf{E}_s$, we can express the imprecision PSD as an overlap integral between the LO and signal mode functions as

$$S_{xx} = \frac{\hbar\omega_0}{8\pi} \frac{1}{P_s} \left(\int_A d\Omega \operatorname{Re} [e_{lo}^* \cdot e_s] \right)^{-2}. \quad (\text{A6})$$

Our task is now to find a mode function e_{lo} which minimizes S_{xx} by maximising the mode overlap with e_s . According to the Cauchy-Schwarz inequality, this maximized overlap is achieved when the LO mode is equal to the signal mode $e_{lo}^{\text{ideal}} = e_s$. We thus find the minimal imprecision noise PSD

$$S_{xx}^{\text{ideal}} = \frac{\hbar\omega_0}{8\pi} \frac{1}{P_s}. \quad (\text{A7})$$

Let us apply this general finding to the problem of orien-

tation detection from the main text. According to Eq. (1), the signal power associated with each of the angles δ and ϵ is given by $P_s = P_0(\Delta\alpha/\alpha_x)^2$, such that Eq. (A7) yields Eq. (6) from the main text.

For a realistic detection system characterized by the (non-ideal) LO mode e_{lo} , the detection efficiency η , defined as the ratio between the ideal imprecision noise S_{xx}^{ideal} and the actual imprecision noise S_{xx} as given by Eq. (A6), is hence

$$\eta = \frac{S_{xx}^{\text{ideal}}}{S_{xx}} = \left(\int_A d\Omega \operatorname{Re} [e_{lo}^* \cdot e_{lo}^{\text{ideal}}] \right)^2. \quad (\text{A8})$$

The detection efficiency is therefore given by the overlap integral between the used LO field e_{lo} and the ideal LO field e_{lo}^{ideal} . We use Eq. (A8) in the main text to determine the realistic detection efficiencies for δ and ϵ in Eqs. (14) and (16).

-
- [1] M. Aspelmeyer, T. Kippenberg, and F. Marquardt, *Cavity Optomechanics: Nano- and Micromechanical Resonators Interacting with Light*, Quantum Science and Technology (Springer Berlin Heidelberg, 2014).
- [2] B. P. Abbott *et al.* (LIGO Scientific Collaboration and Virgo Collaboration), *Phys. Rev. Lett.* **116**, 061102 (2016).
- [3] M. Rossi, D. Mason, J. Chen, Y. Tsaturyan, and A. Schliesser, *Nature* **563**, 53–58 (2018).
- [4] J. Millen, T. S. Monteiro, R. Pettit, and A. N. Vamivakas, *Reports on Progress in Physics* **83**, 026401 (2020).
- [5] R. Reimann, M. Doderer, E. Hebestreit, R. Diehl, M. Frimmer, D. Windey, F. Tebbenjohanns, and L. Novotny, *Phys. Rev. Lett.* **121**, 033602 (2018).
- [6] J. Ahn, Z. Xu, J. Bang, Y. H. Deng, T. M. Hoang, Q. Han, R. M. Ma, and T. Li, *Physical Review Letters* **121**, 033603 (2018).
- [7] J. Ahn, Z. Xu, J. Bang, P. Ju, X. Gao, and T. Li, *Nature Nanotechnology* **15**, 89 (2020).
- [8] J. Bang, T. Seberson, P. Ju, J. Ahn, Z. Xu, X. Gao, F. Robicheaux, and T. Li, *Phys. Rev. Research* **2**, 043054 (2020).
- [9] T. Delord, P. Huillery, L. Nicolas, and G. Hétet, *Nature* **580**, 56 (2020).
- [10] B. A. Stickler, K. Hornberger, and M. S. Kim, *Nature Reviews Physics* (2021), 10.1038/s42254-021-00335-0.
- [11] B. A. Stickler, S. Nimmrichter, L. Martinetz, S. Kuhn, M. Arndt, and K. Hornberger, *Phys. Rev. A* **94**, 033818 (2016).
- [12] B. A. Stickler, B. Schriniski, and K. Hornberger, *Phys. Rev. Lett.* **121**, 040401 (2018).
- [13] B. A. Stickler, B. Papendell, S. Kuhn, B. Schriniski, J. Millen, M. Arndt, and K. Hornberger, *New J. Phys.* **20**, 122001 (2018).
- [14] O. Romero-Isart, *New Journal of Physics* **19**, 123029 (2017).
- [15] A. Manjavacas and F. J. García De Abajo, *Phys. Rev. Lett.* **105**, 113601 (2010).
- [16] R. Zhao, A. Manjavacas, F. J. García De Abajo, and J. B. Pendry, *Phys. Rev. Lett.* **109**, 123604 (2012).
- [17] Z. Xu and T. Li, *Phys. Rev. A* **96**, 033843 (2017).
- [18] A. Manjavacas, F. J. Rodríguez-Fortuño, F. Javier García De Abajo, and A. V. Zayats, *Phys. Rev. Lett.* **118**, 133605 (2017).
- [19] L. Magrini, P. Rosenzweig, C. Bach, A. Deutschmann-Olek, S. G. Hofer, S. Hong, N. Kiesel, A. Kugi, and M. Aspelmeyer, *Nature* **595**, 373 (2021).
- [20] F. Tebbenjohanns, M. L. Mattana, M. Rossi, M. Frimmer, and L. Novotny, *Nature* **595**, 378 (2021).
- [21] F. Tebbenjohanns, M. Frimmer, and L. Novotny, *Phys. Rev. A* **100**, 043821 (2019).
- [22] F. van der Laan, F. Tebbenjohanns, R. Reimann, J. Vijayan, L. Novotny, and M. Frimmer, *Phys. Rev. Lett.* **127**, 123605 (2021).
- [23] C. Zhong and F. Robicheaux, *Phys. Rev. A* **95**, 053421 (2017).
- [24] L. Novotny and B. Hecht, *Principles of Nano-Optics* (Cambridge University Press, 2012).
- [25] W. Bowen and G. Milburn, *Quantum Optomechanics* (Taylor & Francis, 2015).
- [26] We normalize the PSD of a signal $x(t)$ such that $\langle x(t)^2 \rangle = \int_{-\infty}^{\infty} d\omega S_{xx}(\omega)$.
- [27] B. A. Stickler, B. Papendell, and K. Hornberger, *Phys. Rev. A* **94**, 033828 (2016).
- [28] T. Seberson and F. Robicheaux, *Physical Review A* **102**, 033505 (2020), 1909.06469.
- [29] A. Zangwill, *Modern Electrodynamics*, Modern Electrodynamics (Cambridge University Press, 2013).
- [30] C. Cohen-Tannoudji, J. Dupont-Roc, and G. Grynberg, *Photons and Atoms - Introduction to Quantum Electrodynamics* (Wiley, New York, 1989).
- [31] T. W. Marshall, *Proceedings of the Royal Society of London. Series A. Mathematical and Physical Sciences* **276**, 475 (1963).
- [32] T. H. Boyer, *Phys. Rev. D* **11**, 790 (1975).
- [33] A. A. Clerk, M. H. Devoret, S. M. Girvin, F. Marquardt, and R. J. Schoelkopf, *Rev. Mod. Phys.* **82**, 1155 (2010).
- [34] R. G. Barrera, G. A. Estevez, and J. Giraldo, *European Journal of Physics* **6**, 287 (1985).
- [35] B. Carrascal, G. A. Estevez, P. Lee, and V. Lorenzo, *European Journal of Physics* **12**, 184 (1991).
- [36] F. Gittes and C. F. Schmidt, *Opt. Lett.* **23**, 7 (1998).